Sphere Refinement in Gap Safe Screening

Cassio F. Dantas, Emmanuel Soubies, Cédric Févotte

Sphere Refinement in Gap Safe Screening

Cássio F. Dantas, Emmanuel Soubies, Cédric Févotte, *Fellow, IEEE*

***Abstract*—The Gap safe screening technique is a powerful tool to accelerate the convergence of sparse optimization solvers. Its performance is largely based on the ability to determine the smallest "sphere", centered at a given feasible dual point, that contains the dual solution. This can be achieved through an inner sphere refinement loop, applied at each screening step. In this work, we show that this refinement loop actually converges to the solution of a fixed-point equation for which we derive a closed-form expression for two common loss functions. This allows us to develop an analytic (i.e., non iterative) and more elegant variant of the sphere refinement step.**

***Index Terms*—Sparse optimization, Safe screening, Kullback-Leibler regression, Logistic regression.**

I. Introduction

SPARSE optimization problems are encountered in fields such as signal processing, inverse problems, statistics, and machine learning. A very common formulation is given by

$$\mathbf{x}^\star \in \operatorname*{argmin}_{\mathbf{x}\in\mathcal{C}} P_\lambda(\mathbf{x}) := \sum_{i=1}^{m} f_i([\mathbf{A}\mathbf{x}]_i) + \lambda\|\mathbf{x}\|_1 \qquad (1)$$

where $\mathbf{A} \in \mathbb{R}^{m\times n}$, $\mathcal{C} \in \{\mathbb{R}^n, \mathbb{R}^n_{\geq 0}\}$, $\lambda > 0$, and each scalar function $f_i : \mathbb{R} \to \mathbb{R}$ is proper, lower semi-continuous, convex, and differentiable. As such, numerous algorithms have been developed to tackle problems of the form (1). These include, but are not limited to, proximal gradient [1]–[3], coordinate descent [4], [5], and majorization-minimization [6] methods.

Within this context, the promise of safe screening is to identify zero coordinates in $\mathbf{x}^\star$ so as to reduce the size of the problem and, consequently, accelerate the convergence of the solver. This identification can be performed before or within the course of iterations, leading respectively to the so-called static [7] and dynamic [8] screening approaches. Although originally proposed for the Lasso problem [7] (i.e., $f_i(z) = z^2$), safe screening techniques have then been extended to a large variety of sparse-regularized problems [8]–[11]. The case where the ℓ_1-norm in (1) is replaced by a generic group separable norm has also been treated in [9], [12].

Safe Screening in a Nutshell: Safe screening techniques rely on the first-order primal-dual optimality conditions of (1). More precisely, we get the key property that [7], [12]

$$\forall j \in [n],\ |\phi(\mathbf{a}_j^\mathsf{T}\boldsymbol{\theta}^\star)| < 1 \implies x_j^\star = 0, \qquad (2)$$

where $\phi(x) = x$ if $\mathcal{C} = \mathbb{R}^n$ or $\phi(x) = \max(x, 0)$ if $\mathcal{C} = \mathbb{R}^n_{\geq 0}$, and $\boldsymbol{\theta}^* \in \mathbb{R}^m$ is the solution of the dual problem

$$\boldsymbol{\theta}^\star = \operatorname*{argmin}_{\boldsymbol{\theta}\in\Delta_\mathbf{A}} D_\lambda(\boldsymbol{\theta}) := -\sum_{i=1}^{m} f_i^*(-\lambda\theta_i). \qquad (3)$$

This work was supported by the European Research Council (FACTORY, ERC-CoG-6681839), the French ANR (EROSION, ANR-22-CE48-0004) and the NRF in Singapore (DesCartes, CREATE program).

CFD is with TETIS, Université Montpellier, INRAE, Montpellier, France (email: cassio.fraga-dantas@inrae.fr). ES and CF are with IRIT, Université de Toulouse, CNRS, Toulouse, France (e-mail: firstname.lastname@irit.fr).

In the dual formulation (3), f_i^* stands for the Fenchel-Legendre conjugate of f_i while $\Delta_\mathbf{A} = \{\boldsymbol{\theta} \in \mathbb{R}^m \mid \forall j \in [n],\ |\phi(\mathbf{a}_j^\mathsf{T}\boldsymbol{\theta})| \leq 1\} \cap \operatorname{dom}(D_\lambda)$ corresponds to the dual feasible set, with $\operatorname{dom}(D_\lambda)$ the domain of the dual function.

One sees from (2) that the knowledge of $\boldsymbol{\theta}^\star$ allows us to identify zero coordinates in $\mathbf{x}^\star$. Yet, this is not practical as $\boldsymbol{\theta}^\star$ is unknown. The main task in safe screening is thus to define a *safe region* $\mathcal{S} \ni \boldsymbol{\theta}^\star$ from which we can derive the following *safe screening rule* for the jth component

$$\max_{\boldsymbol{\theta}\in\mathcal{S}} |\phi(\mathbf{a}_j^\mathsf{T}\boldsymbol{\theta})| < 1 \implies |\phi(\mathbf{a}_j^\mathsf{T}\boldsymbol{\theta}^\star)| < 1 \implies x_j^\star = 0. \qquad (4)$$

Clearly, in order to maximize screening performance, the safe region $\mathcal{S}$ should be as small as possible (to increase the number of screened variables) while allowing an efficient computation of the *screening test* given by $\max_{\boldsymbol{\theta}\in\mathcal{S}} |\phi(\mathbf{a}_j^\mathsf{T}\boldsymbol{\theta})| < 1$ (to minimize the computational overhead).

Among existing safe regions, the Gap safe sphere [9] leads to state-of-the-art screening performance for a wide range of problems. Given any primal-dual pair $(\mathbf{x}, \boldsymbol{\theta}) \in \mathcal{C}\times\Delta_\mathbf{A}$, it reads as $\mathcal{S} = \mathcal{B}(\boldsymbol{\theta}, \sqrt{2\mathrm{Gap}_\lambda(\mathbf{x}, \boldsymbol{\theta})/\alpha_{\mathbb{R}^m}})$, where $\mathrm{Gap}_\lambda(\mathbf{x}, \boldsymbol{\theta}) = P_\lambda(\mathbf{x}) - D_\lambda(\boldsymbol{\theta}) \geq 0$ and $\alpha_{\mathbb{R}^m} > 0$ corresponds to the strong concavity constant of D_λ over $\mathbb{R}^m$. Not only is its geometry simple (allowing fast screening tests), but its radius vanishes upon convergence of the primal-dual iterates when strong duality holds (i.e., $\mathrm{Gap}_\lambda(\mathbf{x}^\star, \boldsymbol{\theta}^\star) = 0$). Yet, it requires the dual function D_λ to be globally strongly concave which precludes its use for an important class of functions f_i such as the β-divergences with $\beta \in [1, 2)$ [13].

In a previous work [12], we overcame this limitation by computing local strong concavity bounds on well-chosen subsets of the domain. Moreover, by re-evaluating the strong-concavity bound on the current safe sphere, we proposed a sphere refinement loop that improves screening performance.

Contributions: In this letter, we analyze the sphere refinement loop proposed in [12] and recalled in Section II. We prove that it converges to the solution of a fixed-point equation (Proposition 1). This allows us to derive a new algorithm that is exempt of the inner loop, when the fixed-point equation admits a closed-form solution (Alg. 2). We derive in Section IV such closed-from expressions for two popular loss functions: the Kullback-Leibler (KL) divergence and the logistic function. Finally, numerical illustrations and comparisons are reported in Section V.

Notations: Throughout the paper, we let $[n]=\{1, \ldots, n\}$. For a vector $\mathbf{x} \in \mathbb{R}^n$, we denote x_i its ith entry. Given a subset of indices $g \subseteq [n]$ with cardinality $|g| = n_g$, $\mathbf{x}_g \in \mathbb{R}^{n_g}$ stands for the restriction of $\mathbf{x}$ to its elements indexed by g. For a matrix $\mathbf{A}$, we denote $\mathbf{a}_j$ the jth column and $\mathbf{A}_g$ the matrix formed out of the columns of $\mathbf{A}$ indexed by $g \subseteq [n]$. The complement of $\mathcal{A} \subseteq [n]$ is denoted $\mathcal{A}^c = [n] \setminus \mathcal{A}$. Given a

Algorithm 1 GSS with iterative sphere refinement [12]

1: **Inputs:** $\mathbf{x}^0 \in \mathcal{C}$, $\varepsilon_{\text{gap}} > 0$
2: $\mathcal{A} \leftarrow [n]$, $k \leftarrow 1$, $\mathcal{S}^0 \leftarrow \Delta_{\mathbf{A}}$
3: **repeat**
4: ▷ *Primal and Dual updates*
5: $\mathbf{x}^k_{\mathcal{A}} \leftarrow \texttt{PrimalUpdate}(\mathbf{x}^{k-1}_{\mathcal{A}}, \mathbf{A}_{\mathcal{A}})$, $\mathbf{x}^k_{\mathcal{A}^c} \leftarrow \mathbf{0}$
6: $\boldsymbol{\theta}^k \leftarrow \texttt{DualUpdate}(\mathbf{x}^k) \in \Delta_{\mathbf{A}}$
7: ▷ *Safe region with iterative refinement*
8: $\tilde{\mathcal{S}} \leftarrow \mathcal{S}^{k-1}$
9: **if** $\boldsymbol{\theta}^k \notin \tilde{\mathcal{S}}$ **then** ▷ *Inflate previous safe region*
10: $\tilde{\mathcal{S}} \leftarrow \mathcal{B}\left(\boldsymbol{\theta}^{k-1}, \|\boldsymbol{\theta}^k - \boldsymbol{\theta}^{k-1}\|\right)$
11: **end if**
12: $\mathcal{S}^k \leftarrow \mathcal{B}\left(\boldsymbol{\theta}^k, \sqrt{\frac{2\,\text{Gap}_\lambda(\mathbf{x}^k, \boldsymbol{\theta}^k)}{\alpha_{\tilde{\mathcal{S}}}}}\right)$ ▷ *Init. safe region*
13: **if** $\alpha_{\mathcal{S}^k} > \alpha_{\tilde{\mathcal{S}}}$ **then**
14: **repeat** ▷ *Sphere refinement*
15: $\mathcal{S}^k \leftarrow \mathcal{B}\left(\boldsymbol{\theta}^k, \sqrt{\frac{2\,\text{Gap}_\lambda(\mathbf{x}^k, \boldsymbol{\theta}^k)}{\alpha_{\mathcal{S}^k}}}\right)$
16: **until** convergence
17: **end if**
18: ▷ *Screening*
19: $\mathcal{A} \leftarrow \{j \in \mathcal{A} | \max_{\boldsymbol{\theta} \in \mathcal{S}^k} |\phi(\mathbf{a}_j^\intercal \boldsymbol{\theta})| \geq 1\}$
20: $k \leftarrow k + 1$
21: **until** $\text{Gap}_\lambda(\mathbf{x}^k, \boldsymbol{\theta}^k) \leq \varepsilon_{\text{gap}}$

Algorithm 2 Proposed GSS with analytic sphere refinement

1: **Inputs:** $\mathbf{x}^0 \in \mathcal{C}$, $\varepsilon_{\text{gap}} > 0$
2: $\mathcal{A} \leftarrow [n]$, $k \leftarrow 1$, $\mathcal{S}_{\text{b}} \leftarrow \Delta_{\mathbf{A}}$
3: **repeat**
4: ▷ *Primal and Dual updates*
5: $\mathbf{x}^k_{\mathcal{A}} \leftarrow \texttt{PrimalUpdate}(\mathbf{x}^{k-1}_{\mathcal{A}}, \mathbf{A}_{\mathcal{A}})$, $\mathbf{x}^k_{\mathcal{A}^c} \leftarrow \mathbf{0}$
6: $\tilde{\boldsymbol{\theta}} \leftarrow \texttt{DualUpdate}(\mathbf{x}^k) \in \Delta_{\mathbf{A}}$
7: $\boldsymbol{\theta}^k \leftarrow P_{\mathcal{S}_{\text{b}}}(\tilde{\boldsymbol{\theta}})$ ▷ *Projection on* $\mathcal{S}_{\text{b}}$
8: ▷ *Safe region with analytic refinement*
9: $\mathcal{S}^k \leftarrow \mathcal{B}\left(\boldsymbol{\theta}^k, \sqrt{\frac{2\,\text{Gap}_\lambda(\mathbf{x}^k, \boldsymbol{\theta}^k)}{\alpha_{\mathcal{S}_{\text{b}}}}}\right)$ ▷ *Init. safe region*
10: **if** $\|\boldsymbol{\theta}^k - \boldsymbol{\theta}_{\mathcal{S}_{\text{b}}}\| > r_{\mathcal{S}^k} - r_{\mathcal{S}_{\text{b}}}$ **then**
11: **if** $\bar{\alpha}^k > \alpha_{\mathcal{S}_{\text{b}}}$ **then** ▷ $\bar{\alpha}^k$ *fixed-point in* (9)
12: $\mathcal{S}^k \leftarrow \mathcal{B}\left(\boldsymbol{\theta}^k, \sqrt{\frac{2\,\text{Gap}_\lambda(\mathbf{x}^k, \boldsymbol{\theta}^k)}{\bar{\alpha}^k}}\right)$
13: $\mathcal{S}_{\text{b}} \leftarrow \mathcal{S}^k$ ▷ *Track region with best* α
14: **end if**
15: **end if**
16: ▷ *Screening*
17: $\mathcal{A} \leftarrow \{j \in \mathcal{A} | \max_{\boldsymbol{\theta} \in \mathcal{S}^k} |\phi(\mathbf{a}_j^\intercal \boldsymbol{\theta})| \geq 1\}$
18: $k \leftarrow k + 1$
19: **until** $\text{Gap}_\lambda(\mathbf{x}^k, \boldsymbol{\theta}^k) \leq \varepsilon_{\text{gap}}$

subset $\mathcal{S} \subset \mathbb{R}^m$ $\alpha_{\mathcal{S}}$ stands for the strong concavity constant of D_λ over $\mathcal{S}$ (see [12, Proposition 11] for a formal definition). Finally, we will use the acronym GSS for Gap safe screening.

II. GSS with Iterative Sphere Refinement

The Gap safe screening with iterative sphere refinement proposed in [12] is recalled in Alg. 1. There, `PrimalUpdate` (resp., `DualUpdate`) refers to the update step of any iterative primal (resp., dual) solver for (1) (resp., (3)). Then, the construction of the safe region, starting at line 7, is made of three steps.

- First, if the new dual point does not belong to the previous safe region, the latter is inflated (Line 10).
- Second, as $\boldsymbol{\theta}^k \in \tilde{\mathcal{S}}$, Theorem 5 in [12] can be invoked to build a new safe region centered in $\boldsymbol{\theta}^k$ (Line 12).
- Third, if the strong concavity constant over this new safe region improves (Line 13), this safe region is iteratively refined (lines 14–16). From [12, Proposition 7], this refinement loop generates a sequence of nested Gap safe spheres (i.e., with decreasing radius), all centered in $\boldsymbol{\theta}^k$.

Finally, the refined safe region is used at Line 19 to safely screen out zero-coordinates of the solution vector $\mathbf{x}^\star$.

III. GSS with Analytic Sphere Refinement

The proposed Gap safe screening with analytic sphere refinement is presented in Alg. 2. Its main novelties with respect to Alg. 1 are outlined in the next three sections.

A. Tracking the Best Strong Concavity Constant

As opposed to Alg. 1, in Alg. 2 we keep track of the safe region $\mathcal{S}_{\text{b}}$ over which the best (i.e., largest) constant $\alpha_{\mathcal{S}_{\text{b}}}$ has been computed so far. As such, we ensure the construction of a non-decreasing sequence of strong concavity constants. Then, to ensure that the new dual point $\boldsymbol{\theta}^k$ belongs to $\mathcal{S}_{\text{b}}$, we replaced the inflation step at Line 10 of Alg. 1 by the projection step at Line 7 of Alg. 2. The benefit of this modification is twofold.

- It discards the need of recomputing the strong concavity constant (on the inflated region) before refinement.
- It leads to improved dual points. Indeed, given that $\mathcal{S}_{\text{b}}$ is convex and $\boldsymbol{\theta}^\star \in \mathcal{S}_{\text{b}}$, we have for all $\tilde{\boldsymbol{\theta}} \in \Delta_{\mathbf{A}}$

$$\|P_{\mathcal{S}_{\text{b}}}(\tilde{\boldsymbol{\theta}}) - \boldsymbol{\theta}^\star\|_2 \leq \|\tilde{\boldsymbol{\theta}} - \boldsymbol{\theta}^\star\|_2. \tag{5}$$

B. Avoiding Unnecessary Refinement Attempts

In Alg. 2, we added the test at Line 10 to avoid unnecessary refinement attempts. Indeed, one can see that the refinement step will improve the initial kth Gap safe sphere

$$\mathcal{S}^k = \mathcal{B}\left(\boldsymbol{\theta}^k, r^k\right) \quad \text{with} \quad r^k = \sqrt{\frac{2\,\text{Gap}_\lambda(\mathbf{x}^k, \boldsymbol{\theta}^k)}{\alpha_{\mathcal{S}_{\text{b}}}}}, \tag{6}$$

only if $\alpha_{\mathcal{S}^k} > \alpha_{\mathcal{S}_{\text{b}}}$ (i.e., the strong concavity constant on the new $\mathcal{S}^k$ is better than the best one $\alpha_{\mathcal{S}_{\text{b}}}$ computed so far). From the definition of strong concavity,[1] we can thus derive the following three situations (illustrated in Fig. 1 (a-c)),

- *Improvement* if $\mathcal{S}^k \subseteq \mathcal{S}_{\text{b}} \Longrightarrow \alpha_{\mathcal{S}^k} \geq \alpha_{\mathcal{S}_{\text{b}}}$
- *No Improvement* if $\mathcal{S}^k \supseteq \mathcal{S}_{\text{b}} \Longrightarrow \alpha_{\mathcal{S}^k} \leq \alpha_{\mathcal{S}_{\text{b}}}$
- *Indecisive* otherwise.

A typical situation of *improvement* arises when the duality Gap (and thus the radius) decreases more than the displacement of the dual point from one iteration to the next. Indeed,

[1] If a function f is α_1-strongly concave on $\mathcal{S}_1$, then it is $\alpha_2 \geq \alpha_1$ strongly concave on any $\mathcal{S}_2 \subset \mathcal{S}_1$.

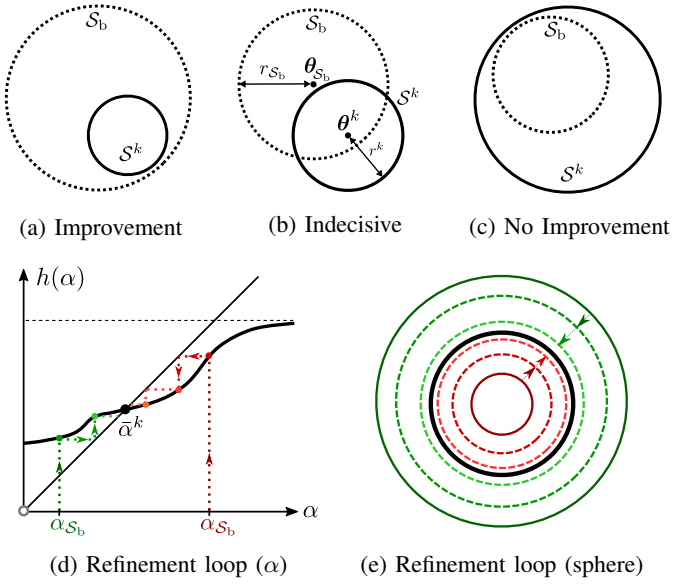

(a) Improvement (b) Indecisive (c) No Improvement

(d) Refinement loop (α) (e) Refinement loop (sphere)

Fig. 1: Sphere refinement behavior. In case (a), computing the fixed point $\bar{\alpha}^k$ would improve over $\alpha_{\mathcal{S}_\mathrm{b}}$. The refinement loop would follow the green path in (d-e). On the contrary, in case (c), computing the fixed point $\bar{\alpha}^k$ would degrade w.r.t. $\alpha_{\mathcal{S}_\mathrm{b}}$. There, running the refinement loop would follow the red path in (d-e). This situation is avoided in Alg. 1 (resp. Alg. 2) by the test at Line 13 (resp. Lines 10-11). Finally, the intermediate case (b) may lead to both mentioned behaviors.

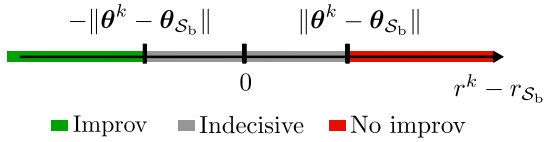

Fig. 2: Illustration of the test at Line 10 of Alg. 2

let $\boldsymbol{\theta}_{\mathcal{S}_\mathrm{b}} \in \Delta_\mathbf{A}$ and $r_{\mathcal{S}_\mathrm{b}} > 0$ denote respectively the center and the radius of $\mathcal{S}_\mathrm{b}$, then $\mathcal{S}^k \subseteq \mathcal{S}_\mathrm{b}$ is equivalent to

$$\|\boldsymbol{\theta}^k - \boldsymbol{\theta}_{\mathcal{S}_\mathrm{b}}\| \leq r_{\mathcal{S}_\mathrm{b}} - r^k. \tag{7}$$

Similarly, we get that $\mathcal{S}^k \supseteq \mathcal{S}_\mathrm{b}$ (i.e., *no improvement* case) is equivalent to

$$\|\boldsymbol{\theta}^k - \boldsymbol{\theta}_{\mathcal{S}_\mathrm{b}}\| \leq r^k - r_{\mathcal{S}_\mathrm{b}}. \tag{8}$$

Hence, the complement of (8) includes all *improvement* and *indecisive* cases (see Fig. 2). It can be used as a test that does not require to compute any strong concavity constant to decide whether to perform the refinement step (Line 10 of Alg. 2). Yet, a second test involving strong concavity constants (Line 11 of Alg. 2) is required to deal with *indecisive* cases.

C. Dropping the Refinement Loop

In Proposition 1, we prove that the sequence of strong concavity constants generated by the refinement loop at lines 14–16 of Alg. 1 converges to the solution $\bar{\alpha}^k$ of a fixed-point equation. This is illustrated in Fig. 1 (d-e). As such, provided that one has access to a closed-form expression for $\bar{\alpha}^k$ (see Section IV), the refinement is no longer iterative, as implemented at Line 12 of Alg. 2.

Proposition 1 (Fixed point equation)**.** *Assume that D_λ is twice differentiable and let $(\mathbf{x}^k, \boldsymbol{\theta}^k) \in \mathcal{C} \times \Delta_\mathbf{A}$ be the kth primal-dual iterate pair and $G^k := \mathrm{Gap}_\lambda(\mathbf{x}^k, \boldsymbol{\theta}^k)$. Moreover let $h : \mathbb{R}_{\geq 0} \to \mathbb{R}_{\geq 0}$ be defined by*

$$h^k(\alpha) = \min_{i \in [m]} \inf_{|\theta_i - \theta_i^k| \leq \sqrt{\frac{2G^k}{\alpha}}} \lambda^2 f_i^{*\prime\prime}(-\lambda\theta_i), \tag{9}$$

where $h^k(0)$ corresponds to the unconstrained inf*. Then, the iterative refinement process (lines 14–16 in Alg. 1) converges to the safe region $\mathcal{S}^k = \mathcal{B}\left(\boldsymbol{\theta}^k, \sqrt{2G^k/\bar{\alpha}^k}\right)$ where $\bar{\alpha}^k$ is an attracting fixed point of h^k.*

Proof. See *Supplementary Material*. □

IV. Closed-Form Expressions of Fixed Points

The practical relevance of Alg. 2 depends on our ability to derive closed-form expressions of fixed points of h^k in (9). We show that this is possible for two very common loss functions.

A. Kullback-Leibler Divergence

Here, the scalar data-fidelity functions f_i and their convex conjugates are given by:

$$f_i(z) = y_i \log\left(y_i/(z+\epsilon)\right) + z + \epsilon - y_i, \tag{10}$$
$$f_i^*(u) = -y_i \log(1-u) - \epsilon u, \tag{11}$$

where y_i is the ith entry of the data vector $\mathbf{y} \in \mathbb{R}^m_{\geq 0}$, $\epsilon > 0$ is a smoothing factor that avoids singularities around zero and $\mathrm{dom}(f_i^*) = \{u \in \mathbb{R} \mid u \leq 1\}$. Finally, in this case we have $\mathcal{C} = \mathbb{R}^n_{\geq 0}$ and $\mathbf{A} \in \mathbb{R}^{m \times n}_{\geq 0}$.

Proposition 2. *Assume that $y_i > 0$ for all $i \in [m]$. Let $(\mathbf{x}^k, \boldsymbol{\theta}^k) \in \mathbb{R}^n_{\geq 0} \times \Delta_\mathbf{A}$ and $G^k := \mathrm{Gap}_\lambda(\mathbf{x}^k, \boldsymbol{\theta}^k)$. Then, h^k in* (9) *with f_i^* in* (11) *has a* unique *attracting fixed-point*

$$\bar{\alpha}^k = \min_{i \in [m]} \bar{\alpha}_i^k \tag{12}$$

$$\text{with } \bar{\alpha}_i^k = \begin{cases} 0 & \text{if } G^k \geq \dfrac{y_i}{2} \\ \dfrac{\lambda^2\left(\sqrt{y_i} - \sqrt{2G^k}\right)^2}{(1+\lambda\theta_i^k)^2} & \text{otherwise.} \end{cases} \tag{13}$$

Proof. See *Supplementary Material*. □

Remark 1. *Following [12, Section 4.4.2], Proposition 2 can be generalized to the situation where there exists $i \in [m]$ such that $y_i = 0$. This is achieved by searching for the* min *in* (12) *within $\mathcal{I}_0^\complement$ rather than $[m]$, where $\mathcal{I}_0 = \{i \in [m] \mid y_i = 0\}$.*

B. Logistic Function

For an input signal $\mathbf{y} \in \mathbb{R}^m$, the data-fidelity functions f_i and their convex conjugates f_i^* are given by:

$$f_i(z) = \log\left(1 + e^z\right) - y_i z \tag{14}$$
$$f_i^*(u) = (y_i + u)\log(y_i + u) + (1 - y_i - u)\log(1 - y_i - u) \tag{15}$$

TABLE I: Proportion of times (%) where $\bar{\alpha}^k \leq \alpha_{\mathcal{S}_\text{b}}$ or $\bar{\alpha}^k > \alpha_{\mathcal{S}_\text{b}}$ for each case of Fig. 1. Bold numbers emphasize the most critical case where $\bar{\alpha}^k$ is computed but not used.

	CoD for Logistic		Prox. Grad. for KL	
	$\bar{\alpha}^k \leq \alpha_{\mathcal{S}_\text{b}}$	$\bar{\alpha}^k > \alpha_{\mathcal{S}_\text{b}}$	$\bar{\alpha}^k \leq \alpha_{\mathcal{S}_\text{b}}$	$\bar{\alpha}^k > \alpha_{\mathcal{S}_\text{b}}$
Improv.	0	89.8	0	44.5
No-Improv.	8.1	0	52.2	0
Indec.	**1.4**	0.7	**2.2**	1.1

with $\text{dom}(f_i^*) = \{u \in \mathbb{R} \mid 0 \leq u + y_i \leq 1\} = [-y_i, 1 - y_i]$. In this case, we have $\mathcal{C} = \mathbb{R}^n$.

Proposition 3. *Let* $(\mathbf{x}^k, \boldsymbol{\theta}^k) \in \mathbb{R}^n \times \boldsymbol{\Delta}_\mathbf{A}$ *and* $G^k := \text{Gap}_\lambda(\mathbf{x}^k, \boldsymbol{\theta}^k)$. *Then* h^k *in* (9) *with* f_i^* *in* (15) *has a* unique *attracting fixed-point*

$$\bar{\alpha}^k = \min_{i \in [m]} \bar{\alpha}_i^k \tag{16}$$

with, for $\tau_i = |\lambda\theta_i^k - y_i + \frac{1}{2}| \leq \frac{1}{2}$,

$$\bar{\alpha}_i^k = \begin{cases} 4\lambda^2 & \text{if } G^k \geq 2\tau_i^2 \\ \dfrac{\lambda^2(2G^k+1)^2}{2G^k} & \text{if } G^k < 2\tau_i^2 \\ & \text{and } \tau_i = \frac{1}{2} \\ \left(\dfrac{-4\tau_i\lambda\sqrt{2G^k} + 2\lambda\sqrt{2G^k + 1 - 4\tau_i^2}}{1 - 4\tau_i^2}\right)^2 & \text{if } G^k < 2\tau_i^2 \\ & \text{and } \tau_i < \frac{1}{2} \end{cases} \tag{17}$$

Proof. See *Supplementary Material*. □

C. Complexity Analysis

The computation of the fixed point from the closed-form expressions derived in propositions 2 and 3 is of the order of $O(m)$ (due to the min operations). This is about the same complexity as for the evaluation of the strong concavity constant on any ball [12, Table 1]. As such, denoting by P the number of sphere refinement iterations in Alg. 1, the analytic version of Alg. 2 allows for reducing the overall sphere refinement complexity from $O(Pm)$ to $O(m)$.

V. Numerical Illustration

In this section, we illustrate the behavior of the sphere refinement procedure with the following two examples:

- KL regression with a proximal gradient (PG) solver [3] for for archetypal analysis on the NIPS papers dataset [14]. The size of the problem is $(m \times n) = (2483 \times 14035)$ and $\lambda = 10^{-2}$.
- Logistic regression with a coordinate descent (CoD) solver [15] for binary classification of the Leukemia dataset [16]. The size of the problem is $(m \times n) = (71 \times 7129)$ and $\lambda = 10^{-1}$.

We report in Table I, for each of the three situations described in Fig. 1, the distribution of times where $\bar{\alpha}^k > \alpha_{\mathcal{S}_\text{b}}$ and $\bar{\alpha}^k \leq \alpha_{\mathcal{S}_\text{b}}$. An interesting observation is that, for both experiments, the proportion of *indecisive* situations is very low (2.1% for Logistic regression with CoD and 3.3% for KL-regression with proximal gradient). In particular, the proportion of times where the fixed point $\bar{\alpha}^k$ has been computed without being used (bold values in Table I) is even smaller. These observations show the efficiency of the simple test at Line 10 of Alg. 2 in discriminating *improvement* from *no-improvement* situations. Note that if, for a given problem, the proportion of *indecisive* cases appears to be more important, and that most of these *indecisive* cases lead to an useless computation of $\bar{\alpha}^k$, it would be preferable to modify the test in Line 10 so as to keep only the *improvement* cases (rather than *improvement* plus *indecisive* cases as in Alg. 2).

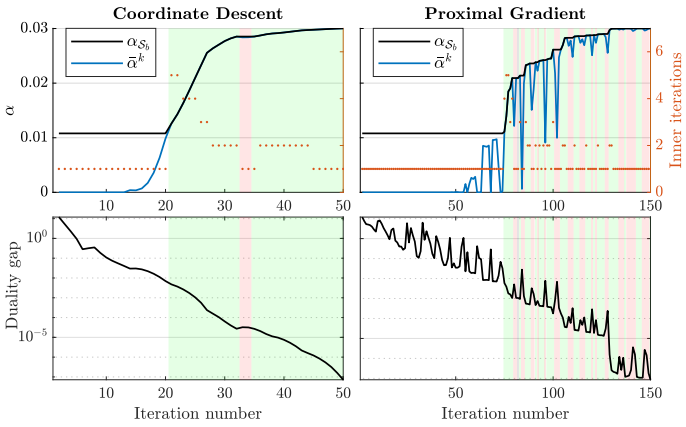

Fig. 3: Evolution of $\bar{\alpha}^k$ and $\alpha_{\mathcal{S}_\text{b}}$ (top) and the duality gap G^k (bottom) as a function of the iteration number k. Green, grey (very rare) and red backgrounds depict respectively the *improvement*, *indecisive*, and *no-improvement* situations. The initial white region correspond to a "burning" phase where $\bar{\alpha}^k < \alpha_{\mathcal{S}_\text{b}} = \alpha_{\boldsymbol{\Delta}_\mathbf{A}}$. Indeed, here $\alpha_{\mathcal{S}_\text{b}}$ has been initialized with $\alpha_{\boldsymbol{\Delta}_\mathbf{A}}$ which is known. The number of inner refinement iterations performed by Alg. 1 is shown in orange.

To further illustrate the sphere refinement behavior, we report in Fig. 3 the evolution of the best strong concavity constant $\alpha_{\mathcal{S}_\text{b}}$, the kth fixed point $\bar{\alpha}^k$, and the duality gap $G^k = \text{Gap}_\lambda(\mathbf{x}^k, \boldsymbol{\theta}^k)$ as a function of the iteration number k. We observe that, in general, *no-improvement* situations (red areas) are associated with a degradation of the duality gap. The occurrence of this phenomenon is directly related to the considered solver and dual update. Moreover, we see that the fixed point $\bar{\alpha}^k$ can be significantly degraded in such *no-improvement* situations (blue curves). This shows the importance of updating the strong concavity constant only when it improves over the current one $\alpha_{\mathcal{S}_\text{b}}$.

The number of refinement iterations performed by Alg. 1 is also reported in Fig. 3. In the coordinate descent (resp. proximal gradient) case, a total of 37 (resp. 69) additional inner iterations are avoided by the proposed approach, including 2 (resp. 33) due to the non-improvement condition.

VI. Conclusion

In this work, we made a theoretical analysis of the sphere refinement loop proposed in [12]. Not only does it shed new light on this refinement step, but it allows us to derive a non-iterative version that is more elegant, more concise, and enjoys a better computational complexity.

REFERENCES

[1] P. Combettes and V. Wajs, "Signal recovery by proximal forward-backward splitting," *Multiscale Modeling & Simulation*, vol. 4, no. 4, pp. 1168–1200, 2005. [Online]. Available: https://doi.org/10.1137/050626090

[2] A. Beck and M. Teboulle, "A fast iterative shrinkage-thresholding algorithm for linear inverse problems," *SIAM Journal on Imaging Sciences*, vol. 2, no. 1, pp. 183–202, Jan 2009. [Online]. Available: http://dx.doi.org/10.1137/080716542

[3] Z. T. Harmany, R. F. Marcia, and R. M. Willett, "This is SPIRAL-TAP: Sparse Poisson Intensity Reconstruction ALgorithms—Theory and Practice," *IEEE Transactions on Image Processing*, vol. 21, no. 3, pp. 1084–1096, March 2012.

[4] W. J. Fu, "Penalized regressions: The bridge versus the lasso," *Journal of Computational and Graphical Statistics*, vol. 7, no. 3, pp. 397–416, 1998. [Online]. Available: http://www.jstor.org/stable/1390712

[5] G.-X. Yuan, K.-W. Chang, C.-J. Hsieh, and C.-J. Lin, "A comparison of optimization methods and software for large-scale l1-regularized linear classification," *Journal of Machine Learning Research*, vol. 11, no. 105, pp. 3183–3234, 2010. [Online]. Available: http://jmlr.org/papers/v11/yuan10c.html

[6] M. A. T. Figueiredo, J. M. Bioucas-Dias, and R. D. Nowak, "Majorization–minimization algorithms for wavelet-based image restoration," *IEEE Transactions on Image Processing*, vol. 16, no. 12, pp. 2980–2991, 2007.

[7] L. El Ghaoui, V. Viallon, and T. Rabbani, "Safe feature elimination for the lasso and sparse supervised learning problems," *Pacific Journal of Optimization*, vol. 8, no. 4, pp. 667–698, Oct 2012, special Issue on Conic Optimization.

[8] A. Bonnefoy, V. Emiya, L. Ralaivola, and R. Gribonval, "Dynamic screening: Accelerating first-order algorithms for the lasso and group-lasso," *IEEE Transactions on Signal Processing*, vol. 63, no. 19, pp. 5121–5132, Oct 2015.

[9] E. Ndiaye, O. Fercoq, A. Gramfort, and J. Salmon, "Gap safe screening rules for sparsity enforcing penalties," *Journal of Machine Learning Research*, vol. 18, no. 128, pp. 1–33, Nov 2017.

[10] J. Wang, Z. Zhang, and J. Ye, "Two-layer feature reduction for sparse-group lasso via decomposition of convex sets," *Journal of Machine Learning Research*, vol. 20, no. 163, pp. 1–42, 2019. [Online]. Available: http://jmlr.org/papers/v20/16-383.html

[11] C. F. Dantas, E. Soubies, and C. Févotte, "Safe screening for sparse regression with the kullback-leibler divergence," in *IEEE International Conference on Acoustics, Speech and Signal Processing (ICASSP)*, Toronto, ON, Canada, June 2021.

[12] ——, "Expanding boundaries of Gap Safe screening," *Journal of Machine Learning Research (JMLR)*, vol. 22, no. 236, pp. 1–57, 2021.

[13] C. Févotte and J. Idier, "Algorithms for nonnegative matrix factorization with the β-divergence," *Neural Computation*, vol. 23, no. 9, p. 2421–2456, Sep 2011. [Online]. Available: https://doi.org/10.1162/NECO_a_00168

[14] A. Globerson, G. Chechik, F. Pereira, and N. Tishby, "Euclidean Embedding of Co-occurrence Data," *The Journal of Machine Learning Research*, vol. 8, pp. 2265–2295, 2007.

[15] P. Tseng and S. Yun, "A coordinate gradient descent method for nonsmooth separable minimization," *Mathematical Programming*, vol. 117, no. 1, pp. 387–423, 2009.

[16] T. R. Golub, D. K. Slonim, P. Tamayo, C. Huard, M. Gaasenbeek, J. P. Mesirov, H. Coller, M. L. Loh, J. R. Downing, M. A. Caligiuri, and C. D. Bloomfield, "Molecular classification of cancer: class discovery and class prediction by gene expression monitoring," *Science*, vol. 286, pp. 531–537, 1999.

SUPPLEMENTARY MATERIAL

A. Proof of Proposition 1

First of all, as D_λ is twice differentiable and separable, we get from [12, Proposition 11] that

$$\alpha_{\mathcal{B}(\boldsymbol{\theta}^k, r^k)} = \min_{i\in[m]} \inf_{|\theta_i - \theta_i^k| \le r^k} \lambda^2 f_i^{*\prime\prime}(-\lambda\theta_i). \tag{18}$$

Then, we know from [12, Proposition 7] that the refinement loop at lines 14–16 of Alg. 1 builds a sequence of nested Gap Safe spheres (i.e., with decreasing radius), all centered in $\boldsymbol{\theta}^k$. With (18), we get that the loop converges to $\bar{\alpha}^k = \alpha_{\mathcal{B}}$ with $\mathcal{B} = \mathcal{B}(\boldsymbol{\theta}^k, \sqrt{\frac{2G^k}{\bar{\alpha}^k}})$, that is an attractive fixed point of h^k.

B. Proof of Propositions 2 and 3

Lemma 1. *Let $h \in C^1$ having a fixed point at $\bar{\alpha}$. Then $\bar{\alpha}$ is attracting if $|h'(\bar{\alpha})| < 1$ and repelling if $|h'(\bar{\alpha})| > 1$.*

Lemma 2. *For $i \in [m]$, let $h_i : \mathbb{R}_{\ge 0} \to \mathbb{R}_{\ge 0}$ be a continuous function that has i) a unique attracting fixed point $\bar{\alpha}_i \ge 0$ and ii) potentially 0 as repelling fixed point. Then $\bar{\alpha} = \min_{i\in[m]} \bar{\alpha}_i$ is the unique attracting fixed point of $h : \alpha \mapsto \min_{i\in[m]} h_i(\alpha)$.*

Proof. By assumption on the h_i, we have $h_i(\bar{\alpha}_i) = \bar{\alpha}_i$ and

$$h_i(\alpha) < \alpha,\ \forall \alpha \in (\bar{\alpha}_i, +\infty) \text{ and } h_i(\alpha) > \alpha,\ \forall \alpha \in (0, \bar{\alpha}_i).$$

Denoting $i^\star = \operatorname{argmin}_{i\in[m]} \bar{\alpha}_i$, we get

$$h(\alpha) \le h_{i^\star}(\alpha) < \alpha,\ \forall \alpha \in (\bar{\alpha}_{i^\star}, +\infty) \tag{19}$$
$$h(\alpha) > \alpha,\ \forall \alpha \in (0, \bar{\alpha}_{i^\star}), \tag{20}$$

The continuity of h_i and h completes the proof. □

Define h_i^k such that h^k in (9) can be written as

$$h^k(\alpha) = \min_{i\in[m]} h_i^k(\alpha). \tag{21}$$

Then, to prove Propositions 2 and 3, it suffices to show that the corresponding h_i^k fulfill the conditions of Lemma 2.

Proof of Proposition 2

We get from [12, Proposition 36] (with $r = \sqrt{2G^k}/\alpha$) that

$$h_i^k(\alpha) := \frac{\lambda^2 y_i \alpha}{\left(\sqrt{\alpha}(1+\lambda\theta_i^k) + \lambda\sqrt{2G^k}\right)^2},$$
$$(h_i^k)'(\alpha) := \frac{\lambda^3 y_i \sqrt{2G^k}}{\left(\sqrt{\alpha}(1+\lambda\theta_i^k) + \lambda\sqrt{2G^k}\right)^3}.$$

In order to invoke Lemma 2, let us analyze the fixed point of h_i^k. Clearly, we always have $h_i^k(0) = 0$ showing that 0 is a fixed point of h_i^k. Moreover, from Lemma 1, it is attracting iff $(h_i^k)'(0) = y_i/(2G^k) < 1 \Leftrightarrow G^k > y_i/2$. Concerning non-zero fixed points, they satisfy

$$\alpha(1+\lambda\theta_i^k)^2 + 2\sqrt{\alpha}(1+\lambda\theta_i^k)\lambda\sqrt{2G^k} + \lambda^2(2G^k - y_i) = 0.$$

This is a quadratic equation in $\sqrt{\alpha}$ with solutions

$$\sqrt{\alpha} = \frac{\lambda(-\sqrt{2G^k} \pm \sqrt{y_i})}{1+\lambda\theta_i^k}. \tag{22}$$

Because $-\sqrt{2G^k} \le 0$, only the "plus" solution is admissible when $G^k < y_i/2$. Moreover, we get from Lemma 1 that $G^k < y_i/2$ also implies that this non-zero fixed point is attracting.

Combining the previous results, we have that

- if $G^k \ge y_i/2$, then h_i^k has a *unique* fixed point, $\bar{\alpha}_i = 0$, which is attracting,
- if $G^k < y_i/2$, then h_i^k has two fixed points: 0 which is repelling and $\bar{\alpha}_i > 0$ (in (22)), which is attracting.

Proof of Proposition 3

Let $\tau_i = |\lambda\theta_i^k - y_i + \frac{1}{2}| \le 1/2$ (the upper bound comes from $\operatorname{dom}(f_i^*(-\lambda\cdot)) = [(y_i-1)/\lambda, y_i/\lambda]$). Then we get from [12, Proposition 23, see proof] (with $r = \sqrt{2G^k}/\alpha$) that

$$h_i^k(\alpha) = \begin{cases} 4\lambda^2 & \text{if } \alpha \le \frac{2\lambda^2 G^k}{\tau_i^2} \\ \frac{4\lambda^2}{1-4\left(\tau_i - \lambda\sqrt{\frac{2G^k}{\alpha}}\right)^2} & \text{if } \alpha \ge \frac{2\lambda^2 G^k}{\tau_i^2} \end{cases}$$

$$(h_i^k)'(\alpha) = \begin{cases} 0 & \text{if } \alpha \le \frac{2\lambda^2 G^k}{\tau_i^2} \\ \frac{16\lambda^3\sqrt{2G^k}\left(\tau_i - \lambda\sqrt{\frac{2G^k}{\alpha}}\right)}{\alpha^{\frac{3}{2}}\left(1-4\left(\tau_i - \lambda\sqrt{\frac{2G^k}{\alpha}}\right)^2\right)^2} & \text{if } \alpha \ge \frac{2\lambda^2 G^k}{\tau_i^2} \end{cases}$$

Note that $(h_i^k)'$ is continuous at $\frac{2\lambda^2 G^k}{\tau_i^2}$ and thus $h_i^k \in C^1$.

Then, from the definition of h_i^k, we distinguish two cases.

• $\bar{\alpha}_i = 4\lambda^2$ is a fixed point of h_i^k if

$$4\lambda^2 \le 2\lambda^2 G^k/\tau_i^2 \iff G^k \ge 2\tau_i^2.$$

Moreover it is attracting (Lemma 1 with $(h_i^k)'(\bar{\alpha}_i) = 0 < 1$).

• Other fixed points of h_i^k are solutions of

$$\alpha(1-4\tau_i^2) + \sqrt{\alpha}8\tau_i\lambda\sqrt{2G^k} - 4\lambda^2(2G^k+1) = 0. \tag{23}$$

– For $\tau_i = \frac{1}{2}$, (23) is a linear equation with solution

$$\sqrt{\bar{\alpha}_i} = \lambda(2G^k+1)/\sqrt{2G^k}. \tag{24}$$

Then, one can check that

$$\bar{\alpha}_i > 8\lambda^2 G^k \iff G^k < 2\tau_i^2 = \frac{1}{2}$$

and $(h_i^k)'(\bar{\alpha}_i) = \frac{1}{2} - G^k < 1$ (i.e., $\bar{\alpha}_i$ is attracting).

– For $\tau_i < \frac{1}{2}$, (23) is a quadratic equation in $\sqrt{\alpha}$ with solutions

$$\sqrt{\alpha} = \frac{-4\tau_i\lambda\sqrt{2G^k} \pm 2\lambda\sqrt{2G^k + 1 - 4\tau_i^2}}{1-4\tau_i^2}. \tag{25}$$

As $\tau_i < \frac{1}{2}$, we have $1-4\tau_i^2 > 0$ and $4\tau_i\lambda\sqrt{2G^k} < 2\lambda\sqrt{2G^k} < 2\lambda\sqrt{2G^k+1-4\tau_i^2}$, showing that the solution with the plus sign is admissible. Denoting $\bar{\alpha}_i$ this solution, we have

$$\bar{\alpha}_i > 2\lambda^2 G^k/\tau_i^2 \iff G^k < 2\tau_i^2.$$

Moreover, one can show that

$$(h_i^k)'(\bar{\alpha}_i) = \frac{\sqrt{2G^k}(2\tau_i\sqrt{2G^k+1-4\tau_i^2} - \sqrt{2G^k})}{1-4\tau_i^2}. \tag{26}$$

is bounded by $\frac{1}{2}(1-\sqrt{1-4\tau_i^2})$ when $G^k < 2\tau_i^2$. Then, with $\tau_i < \frac{1}{2}$, we get that $(h_i^k)'(\bar{\alpha}_i) < \frac{1}{2}$. This shows (with Lemma 1) that $\bar{\alpha}_i$ is attracting. Combining all these disjoint cases complete the proof.